

pubs.acs.org/Macromolecules Article

Investigating the Stress-Strain Behavior in Ring-Opening Metathesis Polymerization-Based Brush Elastomers

Kyle Cushman, Andrew Keith, Joji Tanaka, Sergei S. Sheiko,* and Wei You*



Cite This: Macromolecules 2021, 54, 8365-8371



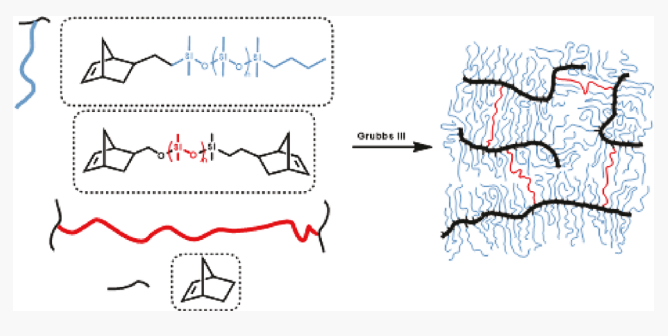
ACCESS

Metrics & More

Article Recommendations

s Supporting Information

ABSTRACT: Brush networks are intriguing materials that are able to replicate the stress—strain behavior of soft tissue, but the effect of the backbone chemical composition on the network mechanics is largely unknown. Here, we show that brush elastomers made by ring-opening metathesis polymerization (ROMP) of norborneneterminated poly(dimethylsiloxane) macromonomers are less extensible than brush elastomers with the methacrylate backbone yet not as extensible (λ_{max}) as predicted by the strain-stiffening parameter (β) derived from fitting the experimental stress—strain curves. The softness (E_0) and firmness (β) of the norbornene-based networks decrease with decreasing cross-link density as



expected, but the λ_{max} significantly drops when the grafting density becomes low enough, which has not been previously observed in this class of materials.

■ INTRODUCTION

Polymeric brush elastomers are an emerging class of synthetic materials that display unique nonlinear elastic character where the materials stiffen with deformation. The mechanical properties of these elastomers are best characterized by tensile stress—strain measurements to determine their "softness" (Young's modulus, E_0) and "firmness" (β). The unique super-softness of brush-like elastomers is enabled by polymeric side chains densely grafted to the backbone, which dilute the network strands and hinder chain entanglements. Place 1,8,9 By contrast, linear polymer-based elastomer networks fail to achieve comparable softness due to the inherent entanglement of network strands.

Similar to linear polymer-based elastomers, the mechanical properties of brush elastomers can be tuned by varying the cross-link density ($\sim n_{\rm x}^{-1}$), where $n_{\rm x}$ is defined as the average number of C–C–C units between cross-links, in the case of most common vinyl monomer-based backbones. However, side chains offer additional mechanical tunability by altering the degree of polymerization of the side chains (SC, $n_{\rm sc}$) and the grafting density ($\sim n_{\rm g}^{-1}$), where $n_{\rm g}$ is the average number of C–C–C units between neighboring grafts (Figure 1). The ratio between $n_{\rm sc}$ and $n_{\rm g}$ dictates the transition between the bottlebrush and comb regimes.

The effects of every architectural parameter $(n_{sc}, n_{g}, \text{ and } n_{x})$ on the stress—strain behavior of polymeric brush elastomers have been extensively studied for methacrylate backbone-based networks (one such example by Sheiko *et al.* is shown in Figure 2), but limited studies feature other classes of backbones. According to computational studies done by Dobrynin *et al.*, conductional properties of graft copolymers with chemically

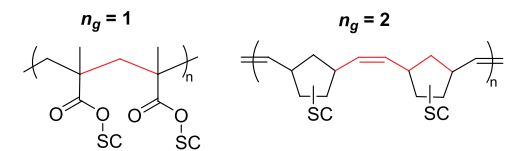


Figure 1. Grafting density defined by the average number of C–C–C units in the backbone between neighboring side chains (SC). The lowest possible $n_{\rm g}$ values for methacrylate and norbornene are 1 and 2, respectively.

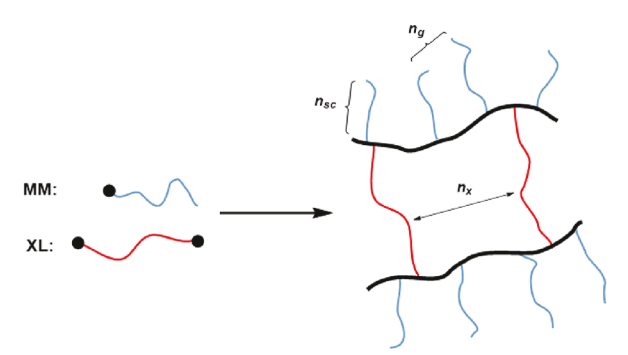
different backbone and side chains may change with stiffer backbones (e.g., poly(norbornene)^{11,12} and cellulose⁵), but the effects of the backbone on brush networks have not been thoroughly examined.

In recent years, ring-opening metathesis polymerization (ROMP) has also been explored for the bottlebrush polymer synthesis, ^{13–20} in particular, owing to the robust functional group tolerance of the catalysts used in ROMP. ^{21–24} Two important features—fast living polymerization kinetics²⁵ and zero-order dependence with respect to catalyst concentration. ²⁶—allow such polymerizations to be carried out at low molar concentration. ²⁷ The latter feature is particularly desirable when polymerizing large macromonomers (MMs)

Received: May 20, 2021 Published: September 7, 2021







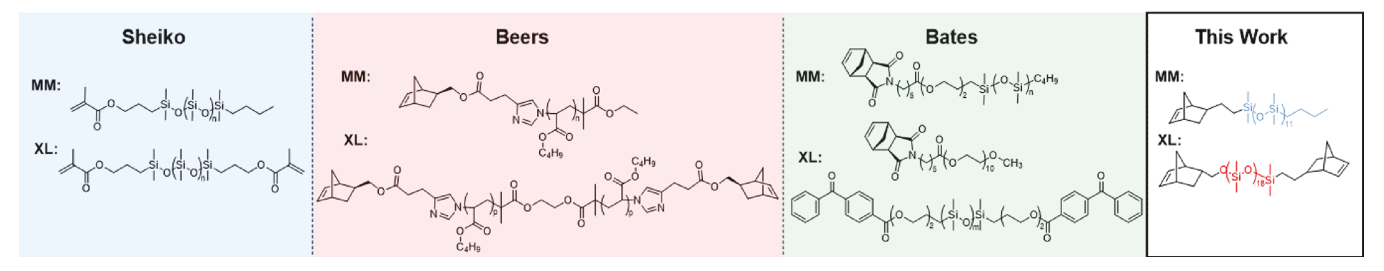


Figure 2. Structural comparison of brush elastomer components of this work to literature studies (Sheiko *et al.*, Beers *et al.*, Beers *et al.*, Degree of polymerization of the side chain (n_{sc}) , grafting-density (n_{g}) , and cross-link density (n_{x}) .

Table 1. Gel Fractions, Swelling Ratio, Extensibility, Modulus, and Strain-Stiffening of the Synthesized Networks

$n_{\rm g}^{a}$	$n_{\rm x}^{b}$	gel fraction ^c (%)	λ_{\max}^{d}	$\lambda_{ m theo}^{e}$	Q^f	G^{g} (kPa)	$G_{\rm e}^{\ h} \ ({\rm kPa})$	E_0^{i} (kPa)	eta^{j}
2	50	80.0	2.1	3.3	11.3	17.2	N/A	59.1	0.093
2	100	84.2	2.3	3.5	12.5	4.3	N/A	14.6	0.080
2	200	92.5	3.3	6.1	16.8	0.2	N/A	0.6	0.027
4	200	98.8	4.5	6.4	17.5	1.3	N/A	3.9	0.024
6	200	96.7	5.7	10.7	19.1	1.4	0.3	5.1	0.009
7	200	90.1	6.9	11.4	20.2	3.2	2.3	16.5	0.008
8	200	90.1	3.6	13.5	20.5	12.0	5.1	51.6	0.006

"Grafting density defined as the ratio of total backbone C–C–C units and C–C–C units containing side chains = 2([NB] + [MM])/[MM]. Effective backbone chain length = 2[MM]/[XL]. Gel fraction determined from the weight of the elastomers before and after washing (see the Supporting Information). Maximum extensibility, experimentally determined. Theoretical extensibility determined from $\lambda_{\text{theo}} = 1/\sqrt{\beta}$ (β from fitting eq 1, last column). Equilibrium swelling ratio in chloroform. Structural shear modulus. Entanglement shear modulus. Young's modulus. Strain-stiffening or firmness parameter.

while still achieving ultralong bottlebrush polymers. Nevertheless, the first demonstration of a ROMP-based brush elastomer was only recently published in 2018 by Beers and co-workers using poly(n-butyl acrylate)(pBA) side chains and a poly(norbornene) backbone (Figure 2). More recently, Bates and co-workers have also reported ROMP-based brush elastomer networks using a universal photo-cross-linking methodology of premade brush melts (Figure 2). However, the effects of architectural parameters (n_{sc} , n_{g} , and n_{x}) on the stress—strain response of such networks have not been studied in these examples.

This study aims to compare the stress—strain response of norbornene-based brush networks (Figure 2) with previously reported methacrylate-based brush networks bearing similar side chains (i.e., similar $n_{\rm sc}$) when altering $n_{\rm x}$ and $n_{\rm g}$. We find that our norbornene-based networks exhibit lower firmness (β) than that of brush networks with the methacrylate backbone, which is ascribed to higher stiffness of poly(norbornene). Furthermore, our networks are less extensible (defined by elongation-at-break $\lambda_{\rm max}$) than predicted from fitted β values ($\lambda_{\rm max} = 1/\sqrt{\beta}$) (Table 1). Decreasing the cross-linking density ($n_{\rm x}$) leads to lower softness (E_0) and firmness (β) and higher extensibility ($\lambda_{\rm max}$) as expected. In addition, increasing the $n_{\rm g}$

(i.e., lower grafting density) resulted in higher λ_{max} ; however, the λ_{max} unexpectedly drops once the grafting density becomes low enough $(n_{\text{g}} = 8)$.

Previous works by Sheiko and co-workers have established a facile one-pot grafting-through strategy to generate bottlebrush elastomers by photoinitiated free-radical polymerization of methacrylate-terminated poly(dimethylsiloxane) (PDMS) macromonomers (MMs) and cross-linkers (XLs). We adopted a similar strategy by using a PDMS-grafted norbornene-based MM and XL to prepare ROMP-based bottlebrush elastomers (Figure 2). In doing so, we largely maintain the chemical structure of the network in previous studies by only switching the PMMA backbone with poly(norbornene) in order to focus on the impact of the backbone on the network mechanics.

■ EXPERIMENTAL SECTION

Materials and Instrumentation. Unless stated otherwise, all reagents were purchased from Sigma-Aldrich, Fisher Scientific, and Gelest and used as received. All NMR spectra were recorded on a 400 MHz spectrometer in CDCl₃ with a solvent residual peak as the internal standard (¹H NMR at 7.26 ppm).

Macromonomer Synthesis. In an oven-dried 250 mL round-bottom flask (RBF) containing a magnetic stirrer, hexamethylcyclotrisiloxane (30.0000 g, 4.48 equiv, 134.86 mmol) was dissolved in

anhydrous hexane (50 mL) and purged with argon. To initiate polymerization, n-butyl lithium (12.041 mL of 2.5 M in hexanes, 1 equiv, 30.102 mmol) was added and then stirred for 1 h before adding tetrahydrofuran (15 mL) as a polymerization promoter. After 3 h, [(5bicyclo [2.2.1] hept-2-enyl) ethyl] dimethylchlorosilane, endo/exo isomers (6.4662 g, 1 equiv, 30.102 mmol), was added, and the reaction was stirred overnight. To remove precipitated lithium chloride and quench any residual n-butyl lithium, the reaction mixture was washed with water (3 × 50 mL), dried with magnesium sulfate, and concentrated via a rotary evaporator. The polymer was precipitated in methanol to remove unreacted monomers and then dried on highvacuum (24.5645 g, 77.56%). The polymer was analyzed by ¹H NMR, and the n_{sc} was determined to be 11. ¹H NMR (400 MHz, CDCl₃) δ : 6.11-5.88 (m, 2H), 2.80-2.73 (m, 2H), 1.96-1.79 (m, 2H), 1.40-1.25 (m, 10 H), 1.22-1.20 (d, 1 H), 1.11-1.03 (m, 2H), 0.90-0.86 (t, 3H), 0.60-0.45 (m, 6H), 0.12-0.01 (m, 66H).

Cross-Linker Synthesis. To an oven-dried 50 mL RBF with a magnetic stirrer, 5-norbornene-2-methanol, endo/exo isomers (0.4184 g, 1 equiv, 3.3697 mmol), was dissolved in 11.3 mL of anhydrous toluene and purged with argon. To this solution, n-butyl lithium (1.35 mL of 2.5 M in hexanes, 1 equiv, 3.3697 mmol) was added dropwise at room temperature and stirred for 10 min. Next, hexamethylcyclotrisiloxane (1.1111 g, 4.9946 mmol) dissolved in 9.37 mL of toluene was purged with argon and then added to the initiator solution. The reaction mixture was allowed to stir for 30 min before introducing a second addition of hexamethylcyclotrisiloxane (3.8889 g, 17.48 mmol) dissolved in 11.06 mL of tetrahydrofuran. Polymerization was allowed to proceed for 3 h, and then [(5-bicyclo[2.2.1]hept-2enyl)ethyl]dimethylchlorosilane, endo/exo isomers (0.7238 g, 1 equiv, 3.3697 mmol), was added, and the reaction was stirred overnight. The mixture was washed with water $(3 \times 25 \text{ mL})$, dried with magnesium sulfate, and concentrated via a rotary evaporator. The cross-linker was precipitated in methanol and dried on high-vacuum (3.9011 g, 70.70%). 1 H NMR analysis was done on the polymer, and the $n_{\rm sc}$ was found to be 18. ¹H NMR (400 MHz, CDCl₃) δ : 6.12–5.88 (m, 4H), 3.76-3.17 (m, 2H), 2.92-2.73 (m, 4H), 1.94-1.74 (m, 2H), 1.62-1.59 (m, 2H), 1.43-1.03 (m, 6H), 0.60-0.42 (m, 4H), 0.11-0.00 (m, 108H).

Bottlebrush Elastomer Polymerization and Purification. The synthesis of the bottlebrush polymer networks was done in a nitrogenfilled glove-box. In a scintillation vial, the mononorborneneterminated poly(dimethylsiloxane) macromonomer (MM) and dinorbornene-terminated poly(dimethylsiloxane) cross-linker (mol $XL = (mol MM/n_x)/2)$ were stirred together until a homogeneous mixture was formed. A 0.1 g/mL solution of a third-generation Grubbs catalyst was formed by dissolving the second-generation Grubbs catalyst M204 (0.0250 g, 0.0294 mmol) in toluene (0.25 mL), adding pyridine (23.7 μ L, 0.294 mmol), and allowing 5 min for ligand exchange to occur. The Grubbs III solution (mol XL/10) was dropped into the polymer mixture, rapidly stirred, and then quickly transferred into a Pyrex glass Petri dish in order to easily cut out dogbones for tensile testing. The network formation appeared to be done within 2 h, but the reaction was left for 18 h to ensure completion. The networks were taken from the glove-box, massed, and then washed with chloroform. Samples were dried in a vacuum oven at 50 °C and massed again to give the gel fraction.

Comb Elastomer Polymerization. Formation of the comb elastomers were done in a nitrogen glove-box. In a scintillation vial, the macromonomer, norbornene (mol NB = $(n_{\rm g}-1) {\rm mol}$ MM), and cross-linker (mol XL = ((mol MM + mol NB)/ $n_{\rm x}$)/2) were mixed together. Grubbs III solution (mol XL/10) was dropped into a separate scintillation vial containing anhydrous toluene (mL Toluene = 1000(mol MM + mol NB)). Such diluted catalyst solution was transferred to the monomer mixture, vigorously mixed, and quickly moved to a glass petri dish. The elastomer appeared to be formed within 1 h and was left to react to completion like the first set. Samples were removed from the glove-box, massed, and then washed with chloroform. Elastomers were dried in a vacuum oven at 50 °C and massed, yielding the gel fraction.

Gel-Fraction Calculation. The gel fraction was determined by measuring the mass before and after chloroform washing. This was calculated using the following formula:

$$\frac{\text{mass of prewash elastomer}}{\text{mass of postwash elastomer}} \times 100 = \text{gel fraction}$$

Dynamic Mechanical Analysis. Samples were cut into dogbones with the bridge dimensions $12 \text{ mm} \times 2 \text{ mm} \times 1 \text{ mm}$ and loaded in an RSA-G2 DMA instrument. Uniaxial extension was done at a constant strain rate of 0.006 s^{-1} and a temperature of $22 \,^{\circ}\text{C}$ until the materials ruptured. The stress—strain curves presented show the dependency of the true stress on the elongation ratio λ , which is classified as the material's extended size L to its initial size L_0 ($\lambda = L/L_0$).

■ RESULTS AND DISCUSSION

Both PDMS-based MMs and XLs were synthesized by anionic ring-opening polymerization (AROP) of hexamethylcyclotrisiloxane to achieve the desired end groups (i.e., norbornene) and chain length $(n_{\rm sc})$. Specifically, the monofunctional norbornene PMDS MMs (1) were prepared using n-butyl lithium as the initiator, which was then end-capped with norbornene species containing an electrophilic chlorosilane moiety (Figure 3). Comparable $n_{\rm sc}$ to the literature was

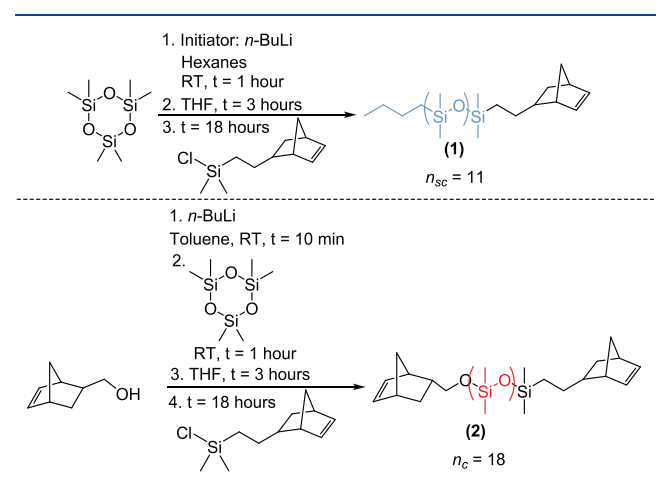


Figure 3. Reaction scheme for anionic ring-opening polymerizations of the mononorbornene PDMS MM (1) and dinorbornene PDMS XL (2).

confirmed by end-group analysis from ¹H NMR spectroscopy $(n_{sc} = 11, Figure S1)$. Using a similar AROP, bifunctional norbornene PMDS XLs (2) were synthesized using the same end-capping strategy but initiated from 5-norbornene-2methanol instead (see the Supporting Information for details). To be consistent with earlier studies,8 we targeted the chain length of the XLs (n_c) to less than three times that of MMs (n_c) = 18 by ¹H NMR, Figure S2). A slight mismatch in reactivity between the MM and cross-linker is expected due to the differences in stereochemistry (exo/endo) and the functional group anchored to the norbornene unit. 14,32,33 In our case, while the ω -end of the XL and the MM bears an exo and endo isomer mixture of the same pendent norbornene functionality, the α -end of the XL has a different exo and endo isomer mixture of norbornene due to the synthetic strategy employed (Figure 3). Given the reported differences in reactivity due to exo/endo isomers and anchor groups (to norbornene), these reactivity differences between the α -end and ω -end of the XL may affect the local cross-link density. 14,34

The brush network by design has three tunable parameters, $n_{\rm sc}$, $n_{\rm g}$, and $n_{\rm x}$. We first investigated the effect of varying the cross-linking density ($n_x = 50$, 100, and 200) with densely grafted bottlebrush networks where each monomer repeat unit contains a side chain. It should be noted that due to the poly(norbornene) monomeric unit length, the highest grafting density possible is roughly twice that of methacrylate (i.e., n_{σ} = 2) (Figure 1). All reactions were carried out in a glove-box to prevent side reactions from oxidations. During our experiments, we found that the synthesis of bottlebrush networks required to be carried out at a near-bulk concentration of MM for higher n_x (i.e., $n_x = 200$). No network formation was observed for n_x above 200, which indicates a lower limit of [XL] to ensure its incorporation into the network via the ROMP of the MM and XL. Using the density of PDMS (0.965 g/mL)³⁵ to calculate the volume of the MM and the ratio of 200 for [MM]/[XL] (for $n_x = 200$), we determined that the lowest possible [XL] in the MM for cross-linking in our system to occur was [XL] = 4.6 mM. Interestingly, Beers and coworkers were able to use a much lower concentration of XL (~0.5 mM in THF) to create their poly(norbornene)-based network.²⁹ We noticed that the length of their XL (22 kg/mol, $n_{\rm sc} \sim 171$) was 5.5 times that of the MM (4 kg/mol, $n_{\rm sc} \sim 31$) $(n_{\rm sc,XL}/n_{\rm sc,MM} = \sim 5.5)$, whereas our XL is just 1.6 times that of the MM ($n_{\rm sc,XL}/n_{\rm sc,MM} = \sim 1.6$). These results indicate that a longer XL could more easily cross-link brushes at low concentration, likely due to the steric repulsion between brush polymers that restricts the accessibility of one brush polymer from the other; a much longer XL (than the length of the MM) would allow easier access to the backbone of another brush polymer. Nevertheless, all the brush elastomers in this set were synthesized at identical bulk concentrations while keeping the ratio of the XL to the Grubbs Gen III catalyst constant ([XL]/[catalyst] = 10). Since ROMP is a living polymerization, 25 the number of catalysts determines the number of propagating polymer chains, and thus the [catalyst] should not theoretically exceed the [XL] to ensure proper formation of the network. Experimentally, each network prepared became rapidly viscous soon after the addition of the catalyst with visible signs of gelation within 2 h. To ensure full monomer conversion, the polymerization was left to continue for 18 h. The gels were then washed with chloroform to remove the unreacted MM and XL and dried in a vacuum oven prior to mechanical testing. The gel fraction was determined from the weight of networks before and after purification in order to ascertain the amount of integrated MM and XL (Table 1).

The gel fraction of these networks $(n_g = 2)$ is higher for lower cross-link densities, i.e., larger n_x (Table 1), which can be ascribed to the reaction required to be conducted at a bulk concentration; a higher concentration of [XL] could promote the propensity of the XL to react with itself, thus being removed during washing. A higher concentration of XL could also cause it to entangle with other XL molecules, which prevents propagating network strands from reaching the reactive XL ends.²⁹ Both factors could contribute to a lower gel fraction. Nonetheless, the gel fractions are all equal to or greater than 80.0%, so the ratio of [MM]/([XL]/2) (as the XL has two norbornene end groups) should provide a decent representation of the true n_x , assuming minimal improper integration of the cross-linker (i.e., intramolecular cyclization). Another qualitative method for gauging the true n_x is by measuring its equilibrium swelling ratio, $Q = V/V_0$, the ratio

between the network volume when swollen with solvent (V) and at the dry state (V_0) , which decreases with increasing cross-link density for our set of networks $(Q = V/V_0 \text{ in Table 1})$.

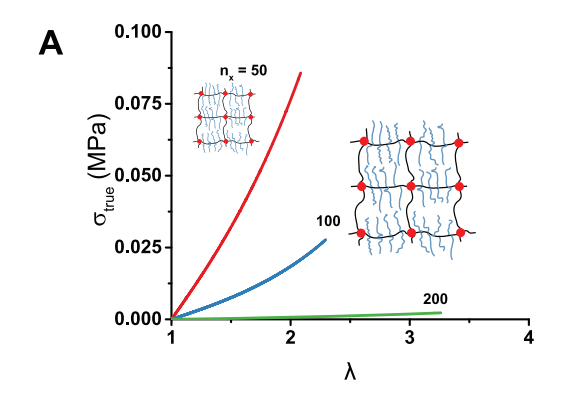
We next evaluated the stress–strain $(\sigma_{\rm true}-\lambda)$ response of the networks by dynamic mechanical analysis (DMA). The softness (E_0) and firmness (β) were determined by fitting stress–strain curves $(\sigma_{\rm true}-\lambda)$ with Dobrynin's equation of state for polymer networks (eq 1):⁸

$$\sigma_{\text{true}} = \frac{G}{3} (\lambda^2 - \lambda^{-1}) \left[1 + \frac{3G_e}{G\lambda} + 2 \left(1 - \frac{\beta(\lambda^2 - 2\lambda^{-1})}{3} \right)^{-2} \right]$$
(1)

where G is the structural shear modulus, $G_{\rm e}$ represents the modulus contribution from entanglements, which can be neglected for dense brushes $(n_{\rm g} \leq 4)$, and β is the strain-stiffening parameter defined as a squared ratio of the initial network strand to the maximum strand end-to-end distance $(\beta = \langle R_{\rm in}^2 \rangle/(R_{\rm max}^2))$, within the interval $0 < \beta < 1$. Each of these values determines Young's modulus $E_0 = G(1 + 2(1 - \beta)^{-2})$, which denotes the linear region of the stress—strain curve at $\lambda \to 1$ ($\lambda = L/L_0$, where L is the extended length to its original length L_0).

Consistent with the general polymer networks' behavior and previous studies, increasing cross-linking density (smaller n_x i.e., shorter network strands) results in a stiffer (higher E_0), firmer (higher β), and less extensible (lower λ_{max}) material (Table 1). Notably, the network made with lowest crosslinking density ($n_x = 200$) with the densest grafting ($n_g = 2$) is remarkably soft, exhibiting lower E_0 (0.59 kPa) than any other reported network made by ROMP. $^{29-31}$ In general, β for each of our networks indicates that they have a weak strainstiffening response (β < 0.1), comparable to the ROMP-based bottlebrush elastomers reported by Bates and co-workers.³⁰ In contrast, methacrylate-based bottlebrush elastomers exhibit a much stronger strain-stiffening character ($\beta > 0.1$).⁸ It is noteworthy that as the mixture of exo and endo norbornene isomers were employed in both MM and XL, exo and endo blocks are expected due to the higher reactivity of the exo isomer over endo.³² However, we do not expect the resulting local spatial differences to make any significant impact on mechanical properties of these network elastomers as such local spatial differences should not affect the global side-chain density.

We next investigated the effect of varying the grafting density ($n_{\rm g}=2$, 4, 6, 7, and 8) using the same cross-linking density ($n_{\rm x}=200$). Polymerization of the networks was carried out as described above, except with the addition of the norbornene (NB) as a comonomer to adjust the $n_{\rm g}$. The total monomer concentration [MM + NB] was lowered to 1 M in toluene because of the higher reactivity of the norbornene spacer to maintain uniform monomer conversion throughout the gel. In our experiments, the viscosity of the reaction mixtures increased rapidly, noticeably with higher norbornene content, and gelation occurred within an hour, but they were left overnight to ensure completion. It is important to note that the reactivity of NB is higher than *exo*-MM and *exo*-XL and even more so when compared to *endo*-MM and *endo*-XL; ³² such reactivity differences may result in uneven distribution of



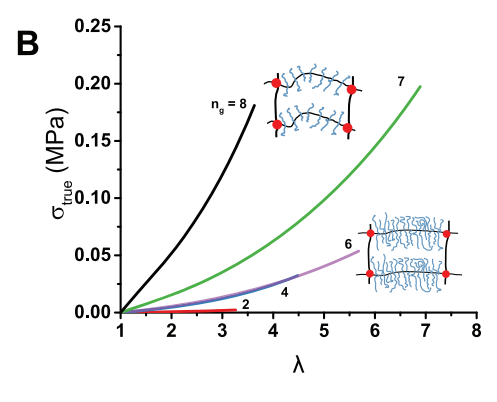


Figure 4. Tensile testing (true-stress, σ_{true} , versus uniaxial elongation, λ) of brush elastomers. (A) Increasing network strand length (n_x) shows a concurrent decrease in softness (E_0) and firmness (β) and an increase in extensibility (λ_{max}) . (B) Decreasing the grafting density (i.e., increase in n_g) increases softness and firmness as well as extensibility until $n_g = 8$ where a significant drop in extensibility is observed.

the side chains throughout the network strands. Here, the $n_{\rm g}$ is considered as the average grafting density. The gel fractions for all of the networks were found to be above 90% (Table 1), comparable to other ROMP brush elastomers. In addition, the networks with reduced grafting density (i.e., higher $n_{\rm g}$) exhibit higher swelling ratios as expected (Table 1). We then examined the mechanical properties of these networks by DMA, and the resulting stress—strain curves (Figure 4B) were fitted with eq 1 without neglecting $G_{\rm e}$ for $n_{\rm g} > 4$.

In general, reducing the grafting density (n_g) results in lower β (Table 1), as expected, as decreasing the side-chain density leads to reduced pre-straining of the backbone. In particular, we observe a significant decrease in β and onset of entanglements (finite G_e) when the grafting density was reduced from $n_g = 4$ to 6, likely indicative of the transition from bottlebrush to comb. Further decreasing the grafting density ($n_g = 7$ and 8) results in noticeably higher moduli (G) with significant contribution from network entanglement (increasing G_e , Table 1). The observed small n_g window for the postulated regime transition from bottlebrush to comb is consistent with the rheology study of ROMP-based molecular polymer brushes reported earlier. 11 Notably, the effect of increasing n_g with norbornene-backbone-based networks results in much lower β values compared to methacrylatebackbone-based ones.⁸ One possible explanation for low β of the poly(norbornene)-based backbone is the tendency of the poly(norbornene) backbone to fold onto itself due to the high crystallinity of the helical backbone, which has been illustrated by Haugan et al. 11 Indeed, Takahashi et al. have previously reported poly(norbornene) to have a helical structure by X-ray crystallography. 37 Furthermore, λ_{\max} increases with increasing $n_{\rm g}$ from 2 to 7, which is expected due to the more coiled backbone conformation in lower grafting density strands. However, we found the λ_{max} to significantly fall for even lower grafting density $(n_g = 8)$; by contrast, in the networks made with methacrylate-terminated PDMS and n-butyl acrylate spacer ($n_{\rm sc}=14,~n_{\rm x}=600$), $\lambda_{\rm max}$ continued to increase with $n_{\rm g}\to32.^8$ Assuming that our networks follow bottlebrush or comb regimes, in theory, the fitted β determines the extensibility of the networks, where $\lambda_{\text{max}} = 1/\sqrt{\beta}$. However, we found the observed λ_{max} to be consistently lower than theoretical λ_{\max} in our poly(norbornene) backbone-based brush networks (Table 1), eluting to the possibility that the theoretical description of bottlebrush and comb regimes might not fully capture poly(norbornene)-based network strands.

Broad dispersity of mesh size could be a possible reason for this, yet further study is required to establish the underlying reason to account for this "unexpected" discovery.

CONCLUSIONS

In summary, our PMDS brush elastomers with a poly-(norbornene) backbone exhibit much lower β values when compared with similar brush elastomers (i.e., n_x and n_g) with a poly(methacrylate) backbone. Sudden transition in β (derived from Dobrynin's model) from n_g = 4 to 6 is likely indicative of the transition between bottlebrush and comb regimes. However, the extensibility ($\lambda_{\rm max}$) of networks appears to be much lower than expected from the theoretical description of bottlebrush or comb regimes. Additionally, there is a significant drop in extensibility at n_g = 8. Further work is necessary to understand the impact of the backbone conformation on stress—strain characters of brush elastomers.

ASSOCIATED CONTENT

Supporting Information

The Supporting Information is available free of charge at https://pubs.acs.org/doi/10.1021/acs.macromol.1c01095.

¹H NMR spectra for the mononorbornene-terminated PDMS macromonomer and dinorbornene-terminated PDMS cross-linker and tensile true stress versus elongation curves with fitting for the studied bottlebrush elastomers (PDF)

AUTHOR INFORMATION

Corresponding Authors

Sergei S. Sheiko — Department of Chemistry, University of North Carolina at Chapel Hill, Chapel Hill, North Carolina 27599, United States; o orcid.org/0000-0003-3672-1611; Email: sergei@email.unc.edu

Wei You — Department of Chemistry, University of North Carolina at Chapel Hill, Chapel Hill, North Carolina 27599, United States; ⊚ orcid.org/0000-0003-0354-1948; Email: wyou@unc.edu

Authors

Kyle Cushman — Department of Chemistry, University of North Carolina at Chapel Hill, Chapel Hill, North Carolina 27599, United States

Andrew Keith — Department of Chemistry, University of North Carolina at Chapel Hill, Chapel Hill, North Carolina 27599, United States; Orcid.org/0000-0001-6351-5392

Joji Tanaka — Department of Chemistry, University of North Carolina at Chapel Hill, Chapel Hill, North Carolina 27599, United States; Orcid.org/0000-0002-2134-8079

Complete contact information is available at: https://pubs.acs.org/10.1021/acs.macromol.1c01095

Author Contributions

The manuscript was written through contributions of all authors. All authors have given approval to the final version of the manuscript.

Notes

The authors declare no competing financial interest.

ACKNOWLEDGMENTS

We acknowledge funding from the National Science Foundation: DMR-1728921 (K.C. and W.Y.), CHE-1808055 (J.T. and W.Y.), DMR-1921835 (A.K. and S.S.), and CHE-0922858 (Bruker AVANCE III Nanobay 400 MHz NMR spectrometer). The authors acknowledge Dr. Marc A. ter Horst and the NMR core for ¹H NMR characterization, Professor Christopher Bates for valuable discussion of physical properties of ROMP-based brush polymer networks, and Jeromy Rech for general project help.

REFERENCES

- (1) Sheiko, S. S.; Dobrynin, A. V. Architectural Code for Rubber Elasticity: From Supersoft to Superfirm Materials. *Macromolecules* **2019**, *52*, 7531–7546.
- (2) Cai, L.-H.; Kodger, T. E.; Guerra, R. E.; Pegoraro, A. F.; Rubinstein, M.; Weitz, D. A. Soft Poly(Dimethylsiloxane) Elastomers from Architecture-Driven Entanglement Free Design. *Adv. Mater.* **2015**, 27, 5132–5140.
- (3) Daniel, W. F. M.; Burdyńska, J.; Vatankhah-Varnoosfaderani, M.; Matyjaszewski, K.; Paturej, J.; Rubinstein, M.; Dobrynin, A. V.; Sheiko, S. S. Solvent-Free, Supersoft and Superelastic Bottlebrush Melts and Networks. *Nat. Mater.* **2016**, *15*, 183–189.
- (4) Reynolds, V. G.; Mukherjee, S.; Xie, R.; Levi, A. E.; Atassi, A.; Uchiyama, T.; Wang, H.; Chabinyc, M. L.; Bates, C. M. Super-Soft Solvent-Free Bottlebrush Elastomers for Touch Sensing. *Mater. Horizons* **2020**, *7*, 181–187.
- (5) Zhang, J.; Keith, A. N.; Sheiko, S. S.; Wang, X.; Wang, Z. To Mimic Mechanical Properties of the Skin by Inducing Oriented Nanofiber Microstructures in Bottlebrush Cellulose- Graft -Diblock Copolymer Elastomers. ACS Appl. Mater. Interfaces 2021, 13, 3278—3286.
- (6) Vatankhah-Varnoosfaderani, M.; Daniel, W. F. M.; Zhushma, A. P.; Li, Q.; Morgan, B. J.; Matyjaszewski, K.; Armstrong, D. P.; Spontak, R. J.; Dobrynin, A. V.; Sheiko, S. S. Bottlebrush Elastomers: A New Platform for Freestanding Electroactuation. *Adv. Mater.* **2017**, 29, 1604209
- (7) Liang, H.; Morgan, B. J.; Xie, G.; Martinez, M. R.; Zhulina, E. B.; Matyjaszewski, K.; Sheiko, S. S.; Dobrynin, A. V. Universality of the Entanglement Plateau Modulus of Comb and Bottlebrush Polymer Melts. *Macromolecules* **2018**, *51*, 10028–10039.
- (8) Vatankhah-Varnosfaderani, M.; Daniel, W. F. M.; Everhart, M. H.; Pandya, A. A.; Liang, H.; Matyjaszewski, K.; Dobrynin, A. V.; Sheiko, S. S. Mimicking Biological Stress—Strain Behaviour with Synthetic Elastomers. *Nature* **2017**, *549*, 497—501.
- (9) Abbasi, M.; Faust, L.; Riazi, K.; Wilhelm, M. Linear and Extensional Rheology of Model Branched Polystyrenes: From Loosely Grafted Combs to Bottlebrushes. *Macromolecules* **2017**, *50*, 5964–5977.

- (10) Liang, H.; Wang, Z.; Sheiko, S. S.; Dobrynin, A. V. Comb and Bottlebrush Graft Copolymers in a Melt. *Macromolecules* **2019**, *52*, 3942–3950.
- (11) Haugan, I. N.; Maher, M. J.; Chang, A. B.; Lin, T.-P.; Grubbs, R. H.; Hillmyer, M. A.; Bates, F. S. Consequences of Grafting Density on the Linear Viscoelastic Behavior of Graft Polymers. *ACS Macro Lett.* **2018**, *7*, 525–530.
- (12) Sarapas, J. M.; Martin, T. B.; Chremos, A.; Douglas, J. F.; Beers, K. L. Bottlebrush Polymers in the Melt and Polyelectrolytes in Solution Share Common Structural Features. *Proc. Natl. Acad. Sci.* **2020**, *117*, 5168–5175.
- (13) Patton, D. L.; Advincula, R. C. A Versatile Synthetic Route to Macromonomers via RAFT Polymerization. *Macromolecules* **2006**, 39, 8674—8683.
- (14) Radzinski, S. C.; Foster, J. C.; Chapleski, R. C., Jr.; Troya, D.; Matson, J. B. Bottlebrush Polymer Synthesis by Ring-Opening Metathesis Polymerization: The Significance of the Anchor Group. *J. Am. Chem. Soc.* **2016**, *138*, 6998–7004.
- (15) Cheng, C.; Khoshdel, E.; Wooley, K. L. Facile One-Pot Synthesis of Brush Polymers through Tandem Catalysis Using Grubbs' Catalyst for Both Ring-Opening Metathesis and Atom Transfer Radical Polymerizations. *Nano Lett.* **2006**, *6*, 1741–1746.
- (16) Choinopoulos, I. Grubbs' and Schrock's Catalysts, Ring Opening Metathesis Polymerization and Molecular Brushes—Synthesis, Characterization, Properties and Applications. *Polymers (Basel)*. **2019**. *11*. 298.
- (17) Teo, Y. C.; Xia, Y. Importance of Macromonomer Quality in the Ring-Opening Metathesis Polymerization of Macromonomers. *Macromolecules* **2015**, *48*, 5656–5662.
- (18) Yu, Y.-G.; Chae, C.-G.; Kim, M.-J.; Seo, H.-B.; Grubbs, R. H.; Lee, J.-S. Precise Synthesis of Bottlebrush Block Copolymers from ω-End-Norbornyl Polystyrene and Poly(4- Tert -Butoxystyrene) via Living Anionic Polymerization and Ring-Opening Metathesis Polymerization. *Macromolecules* **2018**, *51*, 447–455.
- (19) Radzinski, S. C.; Foster, J. C.; Matson, J. B. Preparation of Bottlebrush Polymers via a One-Pot Ring-Opening Polymerization (ROP) and Ring-Opening Metathesis Polymerization (ROMP) Grafting-Through Strategy. *Macromol. Rapid Commun.* **2016**, 37, 616–621.
- (20) Nguyen, H. V. T.; Gallagher, N. M.; Vohidov, F.; Jiang, Y.; Kawamoto, K.; Zhang, H.; Park, J. V.; Huang, Z.; Ottaviani, M. F.; Rajca, A.; et al. Scalable Synthesis of Multivalent Macromonomers for ROMP. ACS Macro Lett. 2018, 7, 472–476.
- (21) Shibuya, Y.; Nguyen, H. V. T.; Johnson, J. A. Mikto-Brush-Arm Star Polymers via Cross-Linking of Dissimilar Bottlebrushes: Synthesis and Solution Morphologies. *ACS Macro Lett.* **2017**, *6*, 963–968.
- (22) Alvaradejo, G. G.; Nguyen, H. V. T.; Harvey, P.; Gallagher, N. M.; Le, D.; Ottaviani, M. F.; Jasanoff, A.; Delaittre, G.; Johnson, J. A. Polyoxazoline-Based Bottlebrush and Brush-Arm Star Polymers via ROMP: Syntheses and Applications as Organic Radical Contrast Agents. ACS Macro Lett. 2019, 8, 473–478.
- (23) Gao, A. X.; Liao, L.; Johnson, J. A. Synthesis of Acid-Labile PEG and PEG-Doxorubicin-Conjugate Nanoparticles via Brush-First ROMP. ACS Macro Lett. 2014, 3, 854–857.
- (24) Radzinski, S. C.; Foster, J. C.; Scannelli, S. J.; Weaver, J. R.; Arrington, K. J.; Matson, J. B. Tapered Bottlebrush Polymers: Cone-Shaped Nanostructures by Sequential Addition of Macromonomers. *ACS Macro Lett.* **2017**, *6*, 1175–1179.
- (25) Jha, S.; Dutta, S.; Bowden, N. B. Synthesis of Ultralarge Molecular Weight Bottlebrush Polymers Using Grubbs' Catalysts. *Macromolecules* **2004**, *37*, 4365–4374.
- (26) Wolf, W. J.; Lin, T.-P.; Grubbs, R. H. Examining the Effects of Monomer and Catalyst Structure on the Mechanism of Ruthenium-Catalyzed Ring-Opening Metathesis Polymerization. *J. Am. Chem. Soc.* **2019**, *141*, 17796–17808.
- (27) Ahn, S.; Pickel, D. L.; Kochemba, W. M.; Chen, J.; Uhrig, D.; Hinestrosa, J. P.; Carrillo, J.-M.; Shao, M.; Do, C.; Messman, J. M.; et al. Poly(3-Hexylthiophene) Molecular Bottlebrushes via Ring-

Opening Metathesis Polymerization: Macromolecular Architecture Enhanced Aggregation. ACS Macro Lett. 2013, 2, 761–765.

- (28) Yamauchi, Y.; Horimoto, N. N.; Yamada, K.; Matsushita, Y.; Takeuchi, M.; Ishida, Y. Two-Step Divergent Synthesis of Monodisperse and Ultra-Long Bottlebrush Polymers from an Easily Purifiable ROMP Monomer. *Angew. Chem., Int. Ed.* **2021**, *60*, 1528–1534.
- (29) Sarapas, J. M.; Chan, E. P.; Rettner, E. M.; Beers, K. L. Compressing and Swelling To Study the Structure of Extremely Soft Bottlebrush Networks Prepared by ROMP. *Macromolecules* **2018**, *51*, 2359–2366.
- (30) Xie, R.; Mukherjee, S.; Levi, A. E.; Reynolds, V. G.; Wang, H.; Chabinyc, M. L.; Bates, C. M. Room Temperature 3D Printing of Super-Soft and Solvent-Free Elastomers. *Sci. Adv.* **2020**, *6*, No. eabc6900.
- (31) Self, J. L.; Sample, C. S.; Levi, A. E.; Li, K.; Xie, R.; de Alaniz, J. R.; Bates, C. M. Dynamic Bottlebrush Polymer Networks: Self-Healing in Super-Soft Materials. *J. Am. Chem. Soc.* **2020**, *142*, 7567–7573.
- (32) Chang, A. B.; Lin, T.-P.; Thompson, N. B.; Luo, S.-X.; Liberman-Martin, A. L.; Chen, H.-Y.; Lee, B.; Grubbs, R. H. Design, Synthesis, and Self-Assembly of Polymers with Tailored Graft Distributions. *J. Am. Chem. Soc.* **2017**, *139*, 17683–17693.
- (33) Lin, T.-P.; Chang, A. B.; Chen, H.-Y.; Liberman-Martin, A. L.; Bates, C. M.; Voegtle, M. J.; Bauer, C. A.; Grubbs, R. H. Control of Grafting Density and Distribution in Graft Polymers by Living Ring-Opening Metathesis Copolymerization. *J. Am. Chem. Soc.* **2017**, *139*, 3896–3903.
- (34) Slugovc, C.; Demel, S.; Riegler, S.; Hobisch, J.; Stelzer, F. The Resting State Makes the Difference: The Influence of the Anchor Group in the ROMP of Norbornene Derivatives. *Macromol. Rapid Commun.* **2004**, *25*, 475–480.
- (35) Mark, J. E. Polymer Data Handbook, 2nd Ed. J. Am. Chem. Soc. **2009**, 131, 16330–16330.
- (36) Keith, A. N.; Clair, C.; Lallam, A.; Bersenev, E. A.; Ivanov, D. A.; Tian, Y.; Dobrynin, A. V.; Sheiko, S. S. Independently Tuning Elastomer Softness and Firmness by Incorporating Side Chain Mixtures into Bottlebrush Network Strands. *Macromolecules* **2020**, *53*, 9306–9312.
- (37) Sakurai, K.; Kashiwagi, T.; Takahashi, T. Crystal Structure of Polynorbornene. *J. Appl. Polym. Sci.* **1993**, 47, 937–940.